Magnetohydrodynamic Free Convection Boundary Layer Flow past A Vertical Cone with Uniform Heat And Mass Flux

S. Gouse Mohiddin[1], O. Anwar Bég[2] and S. Vijaya Kumar Varma[3]

[1]Department of Mathematics, Madanapalle Institute of Technology & Science, Madanapalle – 517325, AP, India
[2]Biomechanics and Biotechnology Research, Aerospace Engineering Program, Mechanical Engineering Subject Group, Sheaf Building, Sheffield Hallam University, Sheffield, S1 1WB, England, UK
[3]Department of Mathematics, Sri Venkateswara University, Tirupati – 517502

Abstract

A numerical solution of unsteady laminar free convection in a viscoelastic fluid flow past a vertical cone with transverse magnetic field applied normal to the surface with uniform heat and mass flux is presented. The Walters-B short-memory liquid model is employed to simulate medical creams and other rheological liquids encountered in biotechnology and chemical engineering. This rheological model introduces supplementary terms into the momentum conservation equation. The dimensionless unsteady, coupled and non-linear partial differential conservation equations for the boundary layer regime are solved by an unconditionally stable implicit finite difference scheme of Crank-Nicolson type. The velocity, temperature and concentration fields have been studied for the effect of viscoelasticity parameter, Prandtl number, magnetic parameter, Schmidt number, and buoyancy ratio parameter and semi vertical angle. The local skin friction, Nusselt number and Sherwood number are also presented and analyzed graphically. The numerical results are validated by comparisons with previously published work and are found to be in excellent agreement.

Key words: cone; finite difference method; flux; Walters-B short-memory model; AMS Subject Classification : 35Q35, 76R10, 76W05. 80A20.

1. Nomenclature

x, y	coordinates along the cone generator and normal to the generator respectively
X, Y	dimensionless spatial coordinates along the cone generator and normal to the generator respectively
u, v	velocity components along the x- and y- directions respectively
U, V	dimensionless velocity components along the X- and Y- directions respectively
Gr_L	Grashof number
g	gravitational acceleration
t'	time
t	dimensionless time
Nu_x	local Nusselt number
Nu_X	non-dimensional local Nusselt number
Pr	Prandtl number
r	local radius of cone
R	dimensionless local radius of the cone
T'	temperature
T	dimensionless temperature
C'	concentration
C	dimensionless concentration
D	mass diffusion coefficient
L	reference length
Sc	Schmidt number
k_0	Walters-B viscoelasticity parameter

Γ dimensionless Walters-B viscoelasticity parameter
N buoyancy ratio parameter
M magnetic parameter
B_0 magnetic field strength
Sh_x local Sherwood number
Sh_X dimensionless local Sherwood number
$f''(0)$ local skin-friction in Ref. [6]

Greek Symbols

β volumetric thermal expansion
μ dynamic viscosity
ν kinematic viscosity
Δt dimensionless time-step
ρ density
α thermal diffusivity
ϕ semi vertical angle of the cone
ΔX dimensionless finite difference grid size in X-direction
ΔY dimensionless finite difference grid size in Y-direction
τ_x local skin friction
τ_X dimensionless local skin-friction
η dimensionless independent variable in [6]
θ temperature in Ref. [6]

Subscripts

w condition on the wall
∞ free stream condition

2. Introduction

Heat and mass transfer in non-Newtonian fluids is of great interest in many operations in the chemical and process engineering industries. Many geometrical configurations have been addressed including flat plates, channels, cones, spheres, wedges, inclined planes and wavy surfaces. The Walters-B viscoelastic model [14] was developed to simulate viscous fluids possessing short memory elastic effects and can simulate accurately many complex polymeric, biotechnological and tribological fluids. The Walters-B model has therefore been studied extensively in many flow problems. One of the first mathematical investigations for such a fluid was presented in [12]. Flat plate thermal convection boundary layer flow of a Walters-B fluid using numerical shooting quadrature was studied in [11]. Exact solutions were obtained in [10] for the combined nonsimilar hydromagnetic flow, heat, and mass transfer phenomena in a conducting viscoelastic Walters-B fluid. Recently theoretical studies on laminar free convection flow of axi-symmetric bodies have received wide attention especially in case of uniform and non-uniform surface heat and mass flux. Similarity solutions for the laminar free convection from a right circular cone were presented in [6]. Reference [8] focused the theoretical study on the effects of suction or injection on steady free convection from a vertical cone with uniform surface heat flux condition. Non-similarity solutions were studied in [5] for the free convection from a vertical permeable cone with non-uniform surface heat flux. Saturated porous media combined heat and mass transfer effects over a full cone was studied in [15].
Magnetohydrodynamic (MHD) flow and heat transfer is of considerable interest because it can occur in many geothermal, geophysical, technological, and engineering applications such as nuclear reactors and others. The geothermal gases are electrically conducting and are affected by the presence of a magnetic field. Vajravelu and Nayfeh [13] studied hydromagnetic convection from a cone and a wedge with variable surface temperature and internal heat generation or absorption. The above studies did not consider combined viscoelastic momentum, heat and mass transfer from a vertical cone, either for the steady case or unsteady case. Owing to the significance of this problem in chemical and medical biotechnological processing (e.g. medical cream manufacture) we study the transient case of such a flow in the present paper using the Walters-B viscoelastic rheological material model.

3. Constitutive Equations For The Walters-B Viscoelastic Fluid

$$p_{ik} = -pg_{ik} + p^*_{ik} \quad (1)$$

$$p^*_{ik} = 2\int_{-\infty}^{t} \Psi\left(t-t^*\right) e^{(1)}_{ik}(t^*)dt^* \quad (2)$$

$$\Psi\left(t-t*\right) = \int_0^{\infty} \frac{N(\tau)}{\tau} e^{\left(-\left(t-t^*\right)/\tau\right)} d\tau \quad (3)$$

where p_{ik} is the stress tensor, p is arbitrary isotropic pressure, g_{ik} is the metric tensor of a fixed coordinate system x_i, $e^{(1)}_{ik}$ is the rate of strain tensor and $N(\tau)$ is the distribution function of relaxation times, τ . The following generalized form of (2) has been shown by Walters [14] to be valid for all classes of motion and stress.

$$p^{*ik}(x,t) = 2\int_{-\infty}^{t} \Psi\left(t-t^*\right) \frac{\partial x^i}{\partial x^{*m}} \frac{\partial x^k}{\partial x^{*r}} e^{(1)mr}\left(x^* t^*\right) dt^* \quad (4)$$

in which $x^*_i = x^*_i(x,t,t^*)$ denotes the position at time t^* of the element which is instantaneously at the position, x_i, at time, t. Liquids obeying the relations (1) and (4) are of the Walters-B' type. For such fluids with short memory i.e. low relaxation times, eqn (4) may be simplified to:

$$p^{*ik}(x,t) = 2\eta_0 e^{(1)ik} - 2k_0 \frac{\partial e^{(1)ik}}{\partial t} \quad (5)$$

in which $\eta_0 = \int_0^{\infty} N(\tau)d\tau$ defines the limiting Walters-B' viscosity at low shear rates, $k_0 = \int_0^{\infty} \tau N(\tau)d\tau$ is the Walters-B' viscoelasticity parameter and $\frac{\partial}{\partial t}$ is the convected time derivative. This rheological model is very versatile and robust and provides a relatively simple mathematical formulation which is easily incorporated into boundary layer theory for engineering applications.

4. Mathematical Model

An axi-symmetric unsteady laminar free convective flow of a viscoelastic fluid past a vertical cone with uniform surface heat and mass flux is considered. Unsteady incompressible flow and non-reactive mass diffusion in a free convective viscoelastic flow driven by species buoyancy force occurs upwards along the cone. Also implicit in our analysis is the assumption that the cone surface and the surrounding fluid which are at rest possess the same temperature T'_∞ and concentration C'_∞ . At time t' >0, heat supplied from the cone surface to the fluid, concentration level near the cone surface are raised at uniform rate and are sustained as constant thereafter. In addition, the formulation of mathematical equations is based on the following assumptions:

- The concentration C' of the diffusing species in the binary mixture is assumed to be very less in comparison to the other chemical species, which are present. This leads to the assumption that the Soret and Dufour effects are negligible.
- The viscous dissipation effects and pressure gradient along the boundary layer are negligible.
- The magnetic Reynolds number is very small so that the induced magnetic field is negligible.
- The magnetic field is not strong enough to cause Joule heating so that the term due to electrical dissipation is neglected in energy equation.

The co-ordinate system chosen (as shown in Fig.1) is such that the *x*- coordinate is directed along the surface of the cone from the apex ($x = 0$) and the *y*- coordinate is orientated perpendicular to this i.e. at right angles to the cone surface, outwards. Here, ϕ designates the semi-vertical angle of the cone and *r* is the local radius of the cone. In compliance with the Boussinesq approximation, all fluid properties are assumed constant except for density variations, which induce *buoyancy* forces, these contributing a dominant, driving role in the free convection regime.

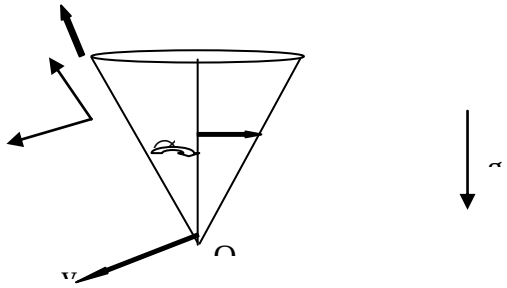

Figure 1: Physical Scenario with Coordinate Axes

Under the above assumptions, implementing the shear-stress strain tensor for a Walters-B liquid, the appropriate unsteady incompressible conservation equations, (neglecting convective inertial terms in the momentum equation) may be shown to take the form: $\frac{\partial(ur)}{\partial x}+\frac{\partial(vr)}{\partial y}=0$

(6) $$\frac{\partial u}{\partial t'}+u\frac{\partial u}{\partial x}+v\frac{\partial u}{\partial y}=\nu\frac{\partial^2 u}{\partial y^2}-k_0\frac{\partial^3 u}{\partial y^2\partial t'}-\frac{\sigma B_0^2}{\rho}u+g\beta\cos\phi(T'-T'_\infty)+g\beta^*\cos\phi(C'-C'_\infty) \quad (7)$$

$$\frac{\partial T'}{\partial t'}+u\frac{\partial T'}{\partial x}+v\frac{\partial T'}{\partial y}=\alpha\frac{\partial^2 T'}{\partial y^2} \quad (8)$$

$$\frac{\partial C'}{\partial t'}+u\frac{\partial C'}{\partial x}+v\frac{\partial C'}{\partial y}=D\frac{\partial^2 C'}{\partial y^2} \quad (9)$$

The initial and boundary conditions are prescribed as:

$$t'\le 0: u=0, v=0, T'=T'_\infty, C'=C'_\infty \quad \text{for all x, y,}$$
$$t'>0: u=0, v=0, T'=T'_w, C'=C'_w \quad \text{at y = 0,}$$
$$u=0, T'=T'_\infty, C'=C'_\infty \quad \text{at x = 0,} \quad (10)$$
$$u\to 0, T'\to T'_\infty, C'\to C'_\infty \quad \text{as } y\to\infty.$$

where all parameters are defined in the nomenclature. Proceeding with analysis, we implement the following non-dimensional quantities to facilitate a numerical solution to the boundary value problem defined by Eqns. (6) to (9) under conditions (10):

$$X=\frac{x}{L}, \qquad Y=\frac{y}{L}(Gr_L)^{\frac{1}{4}}, \qquad R=\frac{r}{L}, \text{where } r=x\sin\phi,$$
$$V=\frac{vL}{\nu}(Gr_L)^{\frac{-1}{4}}, \qquad U=\frac{uL}{\nu}(Gr_L)^{\frac{-1}{2}}, \qquad t=\frac{\nu t'}{L^2}(Gr_L)^{\frac{1}{2}}, \quad (11)$$

$$T=\frac{T'-T'_\infty}{T'_w(L)-T'_\infty},\ Gr_L=\frac{g\beta\left(T'_w(L)-T'_\infty\right)L^3}{\nu^2},\quad \Pr=\frac{\nu}{\alpha},\ M=\frac{\sigma B_0^2L^2}{\mu}Gr_L^{\frac{-1}{2}}$$

$$C=\frac{C'-C'_\infty}{C'_w-C'_\infty},\qquad \Gamma=\frac{k_0Gr_L^{\frac{1}{2}}}{L^2},\quad N=\frac{\beta^*(C'_w-C'_\infty)}{\beta(T'_w-T'_\infty)},\quad Sc=\frac{\nu}{D}$$

Equations (6), (7), (8) and (9) are reduced to the following non-dimensional form

$$\frac{\partial(UR)}{\partial X}+\frac{\partial(VR)}{\partial Y}=0 \tag{12}$$

$$\frac{\partial U}{\partial t}+U\frac{\partial U}{\partial X}+V\frac{\partial U}{\partial Y}=\frac{\partial^2U}{\partial Y^2}-\Gamma\frac{\partial^3U}{\partial Y^2\partial t}-MU+T\cos\phi+NC\cos\phi \tag{13}$$

$$\frac{\partial T}{\partial t}+U\frac{\partial T}{\partial X}+V\frac{\partial T}{\partial Y}=\frac{1}{\Pr}\frac{\partial^2T}{\partial Y^2} \tag{14}$$

$$\frac{\partial C}{\partial t}+U\frac{\partial C}{\partial X}+V\frac{\partial C}{\partial Y}=\frac{1}{Sc}\frac{\partial^2C}{\partial Y^2} \tag{15}$$

The corresponding non-dimensional initial and boundary conditions are given by:

$$\begin{aligned} &t\le 0: U=0, V=0, T=0, C=0 && \text{for all X, Y,} \\ &t>0: U=0, V=0, T=1, C=1 && \text{at Y = 0,} \\ &U=0, \quad T=0, \ C=0 && \text{at X = 0,} \\ &U\to 0, \quad T\to 0, \ C\to 0 && \text{as } Y\to\infty. \end{aligned} \tag{16}$$

Where again all parameters are given in the nomenclature. The dimensionless local values of the skin friction (surface shear stress), the Nusselt number (surface heat transfer gradient) and the Sherwood number (surface concentration gradient) are given by the following expressions:

$$\tau_x=-\left(\frac{\partial U}{\partial Y}\right)_{Y=0} \tag{17}$$

$$Nu_x=-X\left(\frac{\partial T}{\partial Y}\right)_{Y=0} \tag{18}$$

$$Sh_x=-X\left(\frac{\partial C}{\partial Y}\right)_{Y=0} \tag{19}$$

We note that the dimensionless model defined by Eqns. (12) to (15) under conditions (16) reduces to *Newtonian* flow in the case of vanishing viscoelasticity i.e. when $\Gamma\to 0$.

5. Numerical Solution

In order to solve these unsteady, non-linear coupled equations (12) to (15) under the conditions (16), an implicit finite difference scheme of Crank-Nicolson type which is discussed by many authors Muthucumaraswamy and Ganesan [7], Ganesan and Rani [4], Ganesan and Loganathan [3], Prasad et al [9] and Bapuji et al. [1]. The finite difference scheme of dimensionless governing equations is reduced to tri-diagonal system of equations and is solved by Thomas algorithm as discussed in Carnahan et al. [2]. The region of integration is considered as a rectangle with $X_{\max}=1$ and $Y_{\max}=22$ where $Y_{\max}$ corresponds to $Y=\infty$ which lies very well out side both the momentum and thermal boundary layers. The maximum of Y was chosen as 22, after some preliminary investigation so that the last two boundary conditions

of (16) are satisfied within the tolerance limit 10^{-5}. The mesh sizes have been fixed as $\Delta X = 0.05, \Delta Y = 0.05$ with time step $\Delta t = 0.01$. The computations are carried out first by reducing the spatial mesh sizes by 50% in one direction, and later in both directions by 50%. The results are compared. It is observed in all cases, that the results differ only in the fifth decimal place. Hence, the choice of the mesh sizes seems to be appropriate. The scheme is unconditionally stable. The local truncation error is $O(\Delta t^2 + \Delta Y^2 + \Delta X)$ and it tends to zero as $\Delta t, \Delta X$ and ΔY tend to zero. Hence, the scheme is compatible. Stability and compatibility ensure the convergence.

6. Results and Discussion

Only selective figures have been reproduced here for brevity. Default values of the parameters are as follows: viscoelasticity parameter (Γ) = 0.005, buoyancy ratio parameter (N) = 1.0, Schmidt number (Sc) = 0.6 (oxygen diffusing in the viscoelastic fluid), magnetic parameter (M) = 1.0, Prandtl number (Pr) = 0.7 (water-based solvents) and semi-vertical angle of the cone (ϕ) = 20^0. All graphs therefore correspond to these values unless specifically otherwise indicated. In order to prove the accuracy of our numerical results, the present results in steady state at X = 1.0 are obtained by considering the modified Grashof number $Gr_L^* = Gr_L \cos\phi$, (i.e. the numerical solutions obtained from the equations (12) – (15) are independent of semi vertical angle of the cone ϕ)are compared with the available similarity solutions in the literature. The numerical values of local skin friction τ_X, temperature T, for different values of Prandtl number (Pr) are compared with those of Lin [6] in steady state using suitable transformation (i.e. $Y = (20/9)^{1/5}\eta$, $T = (20/9)^{1/5}(-\theta(0))$, $U = (20/9)^{3/5} f'(\eta)$, $\tau_X = (20/9)^{2/5} f''(0)$). It is observed that the results are in good agreement with each other. In addition, the values of local skin friction and temperature are compared with Bapuji et al. [1] for the case of Newtonian fluid in the absence of mass transfer in Table 1 and Table 2.

Table 1 Comparison of steady state local skin-friction values at X = 1.0 with those of Lin [6] and Bapuji et al. [1]

Pr	Lin[6]		Bapuji et al.[1]	Present Results
	$f''(0)$	$\left(\frac{20}{9}\right)^{2/5} f''(0)$	τ_x	
0.72	0.88930	1.2240	1.2154	1.22185
1	0.78446	1.0797	1.0721	1.07476
2	0.60252	0.8293	0.8235	0.82688
4	0.46307	0.6373	0.6328	0.63344
6	0.39688	0.5462	0.5423	0.54362
8	0.35563	0.4895	0.4859	0.48627
10	0.32655	0.4494	0.4460	0.44856
100	0.13371	0.1840	0.1813	0.18291

Table 2 Comparison of steady state temperature values at X = 1.0 with those of Lin [6] and Bapuji et al.[1]

Pr	Lin[6]		Bapuji et al.[1]	Present Results
	$-\theta(0)$	$-\left(\frac{20}{9}\right)^{1/5}\theta(0)$	T	
0.72	1.52278	1.7864	1.7796	1.78084
1	1.39174	1.6327	1.6263	1.62863
2	1.16209	1.3633	1.3578	1.35989
4	0.98095	1.1508	1.1463	1.14895
6	0.89195	1.0464	1.0421	1.04339
8	0.83497	0.9796	0.9754	0.97729
10	0.79388	0.9314	0.9272	0.92832
100	0.48372	0.5675	0.5604	0.56590

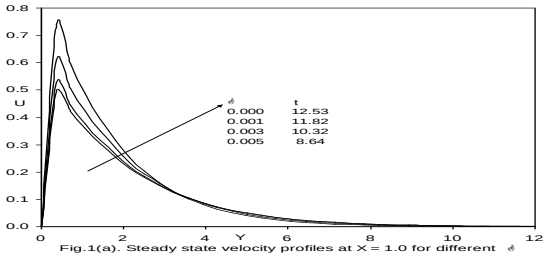

Fig.1(a). Steady state velocity profiles at X = 1.0 for different ϕ

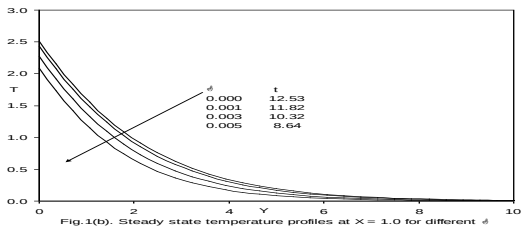

Fig.1(b). Steady state temperature profiles at X = 1.0 for different ϕ

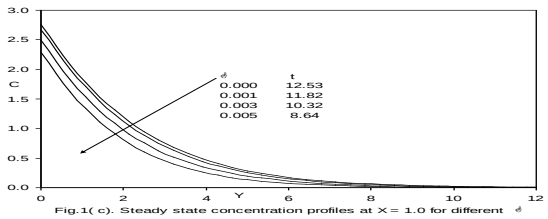

Fig.1(c). Steady state concentration profiles at X = 1.0 for different φ

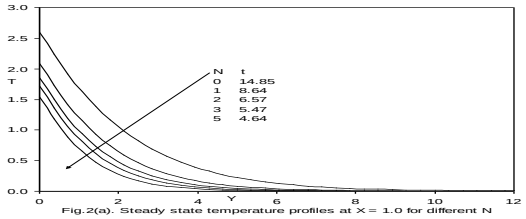

Fig.2(a). Steady state temperature profiles at X = 1.0 for different N

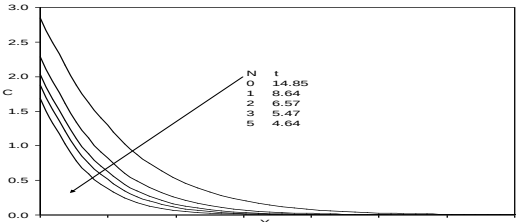

Fig.2(b). Steady state concentration profiles at X = 1.0 for different N

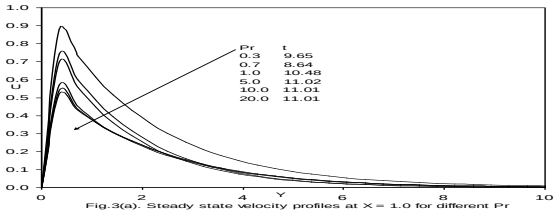

Fig.3(a). Steady state velocity profiles at X = 1.0 for different Pr

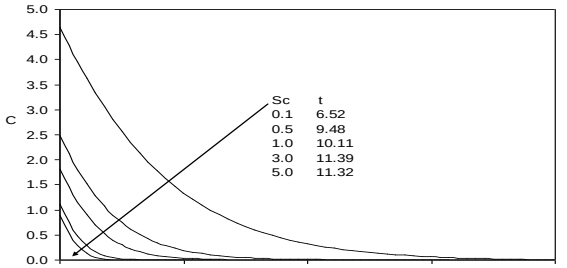

Fig.4.Steady state concentration profiles at X = 1.0 for different Sc

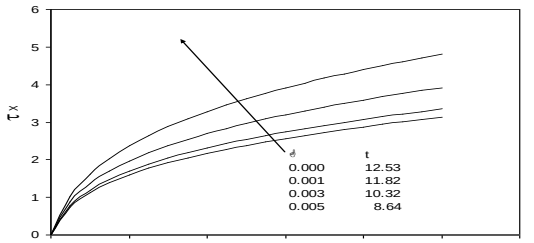

Fig.5(a).Effect of φ on local skin friction

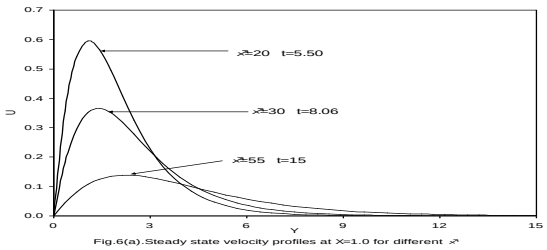

Fig.6(a).Steady state velocity profiles at X=1.0 for different x

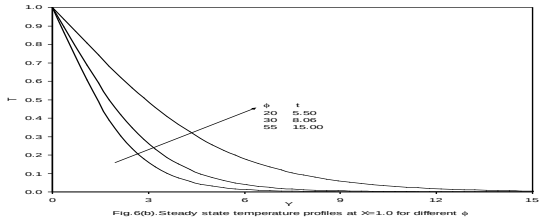

Fig.6(b).Steady state temperature profiles at X=1.0 for different φ

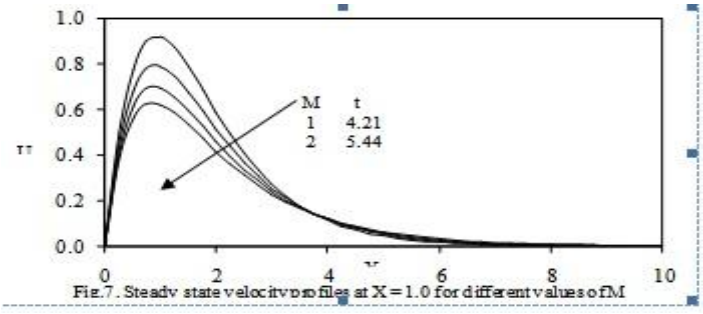

Fig.7. Steady state velocity profiles at X = 1.0 for different values of M

In figures 1a to 1c,

we have presented the variation of streamwise velocity (U), temperature function (T) and concentration (C) versus spanwise coordinate (Y) with collective effects of viscoelasticity (Γ) and time (t), close to the leading edge (i.e. cone apex) at X = 1.0. An increase in Γ from 0 to 0.001, 0.003 and the maximum value of 0.005, as depicted in figure 1a, clearly enhances the streamwise velocity, U which ascends sharply and peaks in close vicinity to the cone surface (Y = 0). In figure 1b increasing viscoelasticity Γ is seen to decrease temperature throughout the boundary layer. The graphs show therefore that increasing viscoelasticity cools the flow. With progression of time, however the temperature, T is consistently enhanced i.e. the fluid is heated as time progresses. A similar response is observed for the concentration field, C, in figure 1c. Increasing viscoelasticity again reduces concentration, showing that species diffuses more effectively in Newtonian fluids (Γ=0) than in strongly viscoelastic fluids. Once again with greater elapse in time the concentration values are reduced throughout the boundary layer regime ($0 < Y < 10$).

In figures 2a and 2b, the distributions of streamwise temperature function (T) and concentration (C) versus spanwise coordinate (Y) for various buoyancy ratio parameters (N) and time (t), close to the leading edge (i.e. cone apex) at X = 1.0, are shown. An increase in N from 0 through 1, 2, 3, 4 to 5 clearly shows that increasing N decrease both temperature (T) and species concentration (C) throughout the boundary layer transverse to the cone surface and that an increase in time has the opposite effect.

Figure 3a illustrate the spanwise spatial response of the velocity U to Prandtl number, Pr and time, t. Increasing Pr from 0.3 through 0.7, 1.0, 5.0, 10.0 to 20.0, clearly reduces strongly streamwise velocity, U (figure 3a) both in the near-wall regime and the far-field regime of the boundary layer. An increase in time, t, also serves to strongly retard the flow.

Figure 4 shows that increase in Sc from 0.1 (low weight diffusing gas species) through 0.5 (oxygen diffusing) to 1.0 (denser hydrocarbon derivatives as the diffusing species), 3.0 and 5.0, strongly *suppresses* concentration levels in the boundary layer regime. All profiles decay monotonically from the cone surface (wall) to the free stream. With a decrease in molecular diffusivity (rise in Sc) concentration boundary layer thickness is therefore decreased.

In **figure 5a** the variation of dimensionless local skin friction (surface shear stress), τ_x, versus streamwise coordinate (X) for various viscoelasticity parameters (Γ) and time (t) are illustrated. Shear stress is clearly enhanced with increasing viscoelasticity.

Figures 6a and 6b

present the spanwise spatial distributions of the U, T variables to semi-apex cone angle, ϕ and time, t. With wider cone angles i.e. a rise from 20 through 30 to 55 degrees (cone apex angle = 2ϕ =110 degrees), the velocity profiles are considerably reduced close to the cone surface i.e. the flow is strongly decelerated near the wall. With further transverse locations from the wall into the boundary layer, however this trend is reversed and streamwise velocity, U, is marginally greater than for smaller cone angles. With grater elapse of time from t = 5.0 through 8.06 to 15, the flow is also found to decelerate. Conversely in figure 6b, an increasingly wider cone apex, induces greater temperatures continuously throughout the boundary layer i.e. heats the boundary layer regime. With progression of time, T values are also increased.
Finally in **Figures 7** the influence of magnetic parameter (M) versus spanwise spatial distributions of velocity U are depicted. Application of magnetic field normal to the flow of an electrically conducting fluid gives rise to a resistive force that acts in the direction opposite to that of the flow. This force is called the Lorentz force. This resistive force tends to slow down the motion of the fluid along the cone and causes an increase in its temperature and a decrease in velocity as M increases. An increase in M from 1 though 2, 3, 4 clearly reduces streamwise velocity U both in the near-wall regime and far-field regime of the boundary layer.

7. Conclusions

A two-dimensional unsteady laminar incompressible boundary layer model has been presented for the external flow, heat and mass transfer in viscoelastic buoyancy driven convection regime past a vertical stationary cone. The Walters-B viscoelastic model has been employed which is valid for short memory polymeric fluids. The dimensionless conservation equations have been solved with the well-tested implicit crank-Nicolson finite difference numerical method. Present results are compared with the available results from the open literature and found to be in very good agreement. The following conclusions are drawn.
Increasing viscoelasticity accelerates the streamwise velocity and enhances shear stress (Local skin friction). Local Nusselt number and local Sherwood number but reduce temperature and concentration values transverse to the cone surface (i.e. inside the boundary layer regime).

- An increase in cone apex angle is found to strongly decelerate the flow near the cone surface but to increase temperature in the boundary layer regime.
- The flow is considerably accelerated close to the wall with a positive increase in buoyancy ratio parameter, corresponding to the case where both thermal and species buoyancy forces assist each other in the regime. The steady state response for the flow is also studied in detail.
- An increase in Schmidt number is observed to significantly decrease concentration.
- The time taken to reach steady state increases with increasing Prandtl number.
- An increase in Prandtl number is observed to reduce both velocity, temperature but increase concentration. The Momentum, Thermal boundary layers becomes thin when Pr is increased.

References

[1] Bapuji Pullepu, Ekambavanan, K., Chamkha, A. J., Unsteady laminar free convection from a vertical cone with uniform surface heat flux, Nonlinear Analysis: Modelling and Control. 13 (2008) 47-60.

[2] Carnahan, B., Luther, H. A., Wilkes, J.O., Applied Numerical Methods, John Wiley and Sons, New York (1969).

[3] Ganesan, P., Loganathan, P., Unsteady natural convection flow past a moving vertical cylinder with heat and mass transfer, Heat Mass Transf., 37 (2001) 59-65.

[4] Ganesan, P., Rani, H. P., Unsteady free convection MHD flow past a vertical cylinder with heat and mass transfer, Int. J. Therm. Sci., 39 (2000) 265-272.

[5] Hossain, M. A., Paul, S. C., Mandal, A. C., Natural convection flow along a vertical circular cone with uniform surface temperature and surface heat flux in a thermally stratified medium, International Journal of Numerical Methods for Heat and Fluid Flow, 12 (2002) 290-305.

[6] Lin, F. N., Laminar convection from a vertical cone with uniform surface heat flux, Letters in Heat and Mass Transfer, 3 (1976) 49-58.

[7] Muthucumaraswamy, R., Ganesan, P., Unsteady flow past an impulsively started vertical plate with heat and mass transfer, Heat Mass Transf., 34 (1998) 187-193.

[8] Pop, I., Watanabe, T., Free convection with uniform suction or injection from a vertical cone for constant wall heat flux, Int. Comm. Heat Mass Transfer, 19 (1992) 275-283.

[9] Prasad, V. R., Bhaskar Reddy, N., Muthucumaraswamy, R., Radiation and mass transfer effects on two dimensional flow past an impulsively started infinite vertical plate, Int. J. Thermal Sciences., 46 (2007) 1251-1258.

[10] Rajagopal, K., Veena, P. H., Pravin, V. K., Nonsimilar Solutions for heat and mass transfer flow in an electrically conducting viscoelastic fluid over a stretching sheet saturated in a porous medium with suction/blowing, J. Porous Media, 11 (2008) 219–230.

[11] Raptis, A. A., Takhar, H. S., Heat transfer from flow of an elastico-viscous fluid, Int. Comm. Heat and Mass Transfer, 16 (1989) 193–197.

[12] Soundalgekar, V. M., Puri, M., On fluctuating flow of an elastico-viscous fluid past an infinite plate with variable suction, J. Fluid Mechanics, 35 (1969) 561–573.

[13] Vajravelu K & Nayfeh L, Hydromagnetic convection at a cone and a wedge, Int Commun Heat Mass Transfer, 19 (1992) 701–710.

[14] Walters, K., Non-Newtonian effects in some elastico-viscous liquids whose behaviour at small rates of shear is characterized by a general linear equation of state, Quart. J. Mech. Applied. Math., 15 (1962) 63–76.

[15] Yih, K. A., Coupled heat and mass transfer by free convection over a truncated cone in porous media: VWT/VWC or VHF/VMF, Acta Mechanica, 137 (1999) 83-97.